

## Supporting information

### Improving the efficiency of P3HT:perylene diimide solar cells via bay-substitution with fused aromatic rings

Erika Kozma,<sup>\*a</sup> Dariusz Kotowski,<sup>a</sup> Silvia Luzzati,<sup>a</sup> Marinella Catellani,<sup>a</sup> Fabio Bertini,<sup>a</sup> Antonino Famulari,<sup>b</sup> and Guido Raos<sup>b</sup>

### Materials and instruments

10-nonadecanone was purchased from TCI Europe. Sodium bis(2-methoxyethoxy) aluminium hydride (RedAl), perylene-3,4,9,10-tetracarboxylic dianhydride, naphthalene-1-boronic acid, acenaphthene-5-boronic acid, tetrakis(triphenylphosphine)palladium(0) were purchased from Aldrich and used as received without further purification. Solvents and reagents were dried and/or distilled by the usual methods and typically used under an inert gas atmosphere.

<sup>1</sup>H-NMR spectra were recorded on a 400 MHz Bruker spectrometer operating at 11.7 T. Thermogravimetric analysis (TGA) was performed on a Perkin-Elmer TGA 7 instrument with a platinum pan using 1.5-2 mg of material as probe. Before performing TGA run, the sample was held at 50 °C for 1 h; the runs were carried out at heating rate of 10 °C min<sup>-1</sup> in a nitrogen atmosphere at a flow rate of 35 ml min<sup>-1</sup>. TGA was recorded from 50 up to 700 °C.

Differential Scanning Calorimetry (DSC) measurements were carried out on a Perkin-Elmer Pyris 1 instrument equipped with a liquid nitrogen device. The sample, typically 2-3 mg, was placed in a sealed aluminum pan and the measurements were carried out from 0 to 200 °C under helium atmosphere using heating and cooling rates of 10 °C min<sup>-1</sup>.

Cyclic voltammetry measurements were performed in solid state, under nitrogen atmosphere with a computer controlled Amel 2053 (with Amel 7800 interface) electrochemical workstation in a three electrode single-compartment cell using platinum electrodes and SCE as standard electrode, ferrocene as internal standard, with a tetrabutylammonium tetrafluoroborate solution (0.1M) in acetonitrile.

Electronic absorption spectra were performed with a Perkin Elmer Lambda 9 spectrophotometer on chloroform solutions or spin coated films on quartz. Photoluminescence (PL) spectra were recorded using 450 nm light excitation from a xenon lamp and a monochromator coupled to a N<sub>2</sub> cooled CCD detector.

## Reaction scheme and synthetic procedures

The synthetic procedures for the preparation of 10-nonadecanamine, PDI-1 and 1, 7-dibromo-N,N'-bis-(10-nonadecyl)-perylene-3,4,9,10-bis(dicarboximide) were described elsewhere [1].

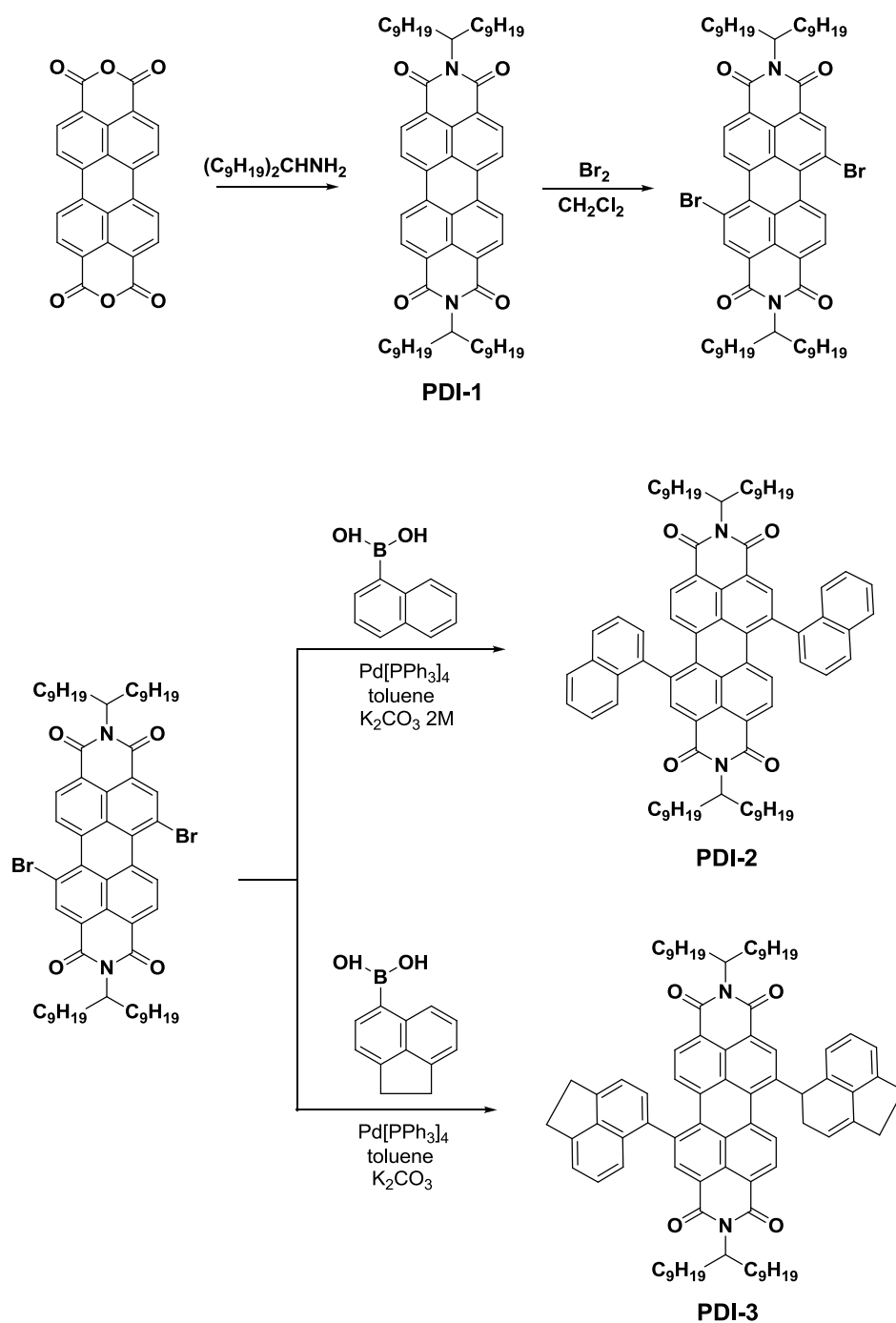


**Figure 1.** Synthetic route toward **PDI-1**, **PDI-2** and **PDI-3**

Synthesis of 1, 7-bis(1-naphthalenyl)-N,N'-bis-(10-nonadecyl)-perylene-3,4,9,10-bis(dicarboximide) **PDI-2**

A mixture of 1,7-dibromo-N,N'-bis(10-nonadecyl)perylene-3,4,9,10-tetracarboxylic diimide [1] and naphthalene-1-boronic acid (2.04 equivalents) were dissolved in dry toluene (5 ml each 0.25 mmol of dibromo-N,N'-bis(nonadecyl)perylene-3,4,9,10-tetracarboxylic diimide) and 2M K<sub>2</sub>CO<sub>3</sub> solution (1 ml each 4 ml of toluene). Catalytic amounts of Pd[PPh<sub>3</sub>]<sub>4</sub> were added and the reaction mixture was stirred at 100<sup>0</sup>C for 18 hours. Shortly after the addition of the catalyst, the colour of the mixture starts to change. At the end of the reaction time, the solution was cooled to room temperature, extracted with CHCl<sub>3</sub>, washed with water, extracted and dried over MgSO<sub>4</sub> anh. concentrated to a smaller volume and dropped into methanol. The precipitate was filtered, and further purified by column chromatography, using hexane/CHCl<sub>3</sub> 3:2 as eluent.

1, 7-bis(1-naphthalenyl)-N,N'-bis-(10-nonadecyl)-perylene-3,4,9,10-bis(dicarboximide) **PDI-2** was obtained as a deep red solid in 78% yield. <sup>1</sup>H-NMR(CDCl<sub>3</sub>, 400MHz): δ = 8.64 (2H, m, pery), 8.00 (4H, dd, pery), 7.62 (6H, m, naph), 7.52 (4H, t, naph), 7.31 (4H, t, naph), 5.10 (2H, m, -CH-N), 2.20 (4H, m, -CH<sub>2</sub>-), 1.80 (4H, m, -CH<sub>2</sub>-), 1.22 (56H, m, -CH<sub>2</sub>-), 0.81 (12H, t, -CH<sub>3</sub>).

Synthesis of 1, 7-bis(5-acenaphtenyl)-N,N'-bis-(10-nonadecyl)-perylene-3,4,9,10-bis(dicarboximide) **PDI-3**

A mixture of 1,7-dibromo-N,N'-bis(10-nonadecyl)perylene-3,4,9,10-tetracarboxylic diimide [1] and acenaphthene-5-boronic acid (2.04 equivalents) were dissolved in dry toluene (5 ml each 0.25 mmol of dibromo-N,N'-bis(nonadecyl)perylene-3,4,9,10-tetracarboxylic diimide) and 2M K<sub>2</sub>CO<sub>3</sub> solution (1 ml each 4 ml of toluene). Catalytic amounts of Pd[PPh<sub>3</sub>]<sub>4</sub> were added and the reaction mixture was stirred at 100<sup>0</sup>C for 18 hours. Shortly after the addition of the catalyst, the colour of the mixture starts to change. At the end of the reaction time, the solution was cooled to room temperature, extracted with CHCl<sub>3</sub>, washed with water, extracted and dried over MgSO<sub>4</sub> anh. concentrated to a smaller volume and dropped into methanol. The precipitate was filtered, and further purified by column chromatography, using hexane/CHCl<sub>3</sub> 3:2 as eluent.

1, 7-bis(5-acenaphtenyl)-N,N'-bis-(10-nonadecyl)-perylene-3,4,9,10-bis(dicarboximide) **PDI-3** was obtained as a deep violet solid in 63% yield. <sup>1</sup>H-NMR (TCE, 400MHz): δ = 8.61 (2H, m, pery), 7.90 (4H, m, pery), 7.58 (2H, m, acenaph), 7.35 (4H, m, acenaph), 7.25 (4H, m, acenaph), 5.05 (2H, m, -CH-N), 3.45 (8H, m, -CH<sub>2</sub>- acenaph), 2.05 (4H, m, -CH<sub>2</sub>-), 1.73 (4H, m, -CH<sub>2</sub>-), 1.12 (56H, m, -CH<sub>2</sub>-), 0.78 (12H, t, -CH<sub>3</sub>).

### TGA of PDI-2 and PDI-3

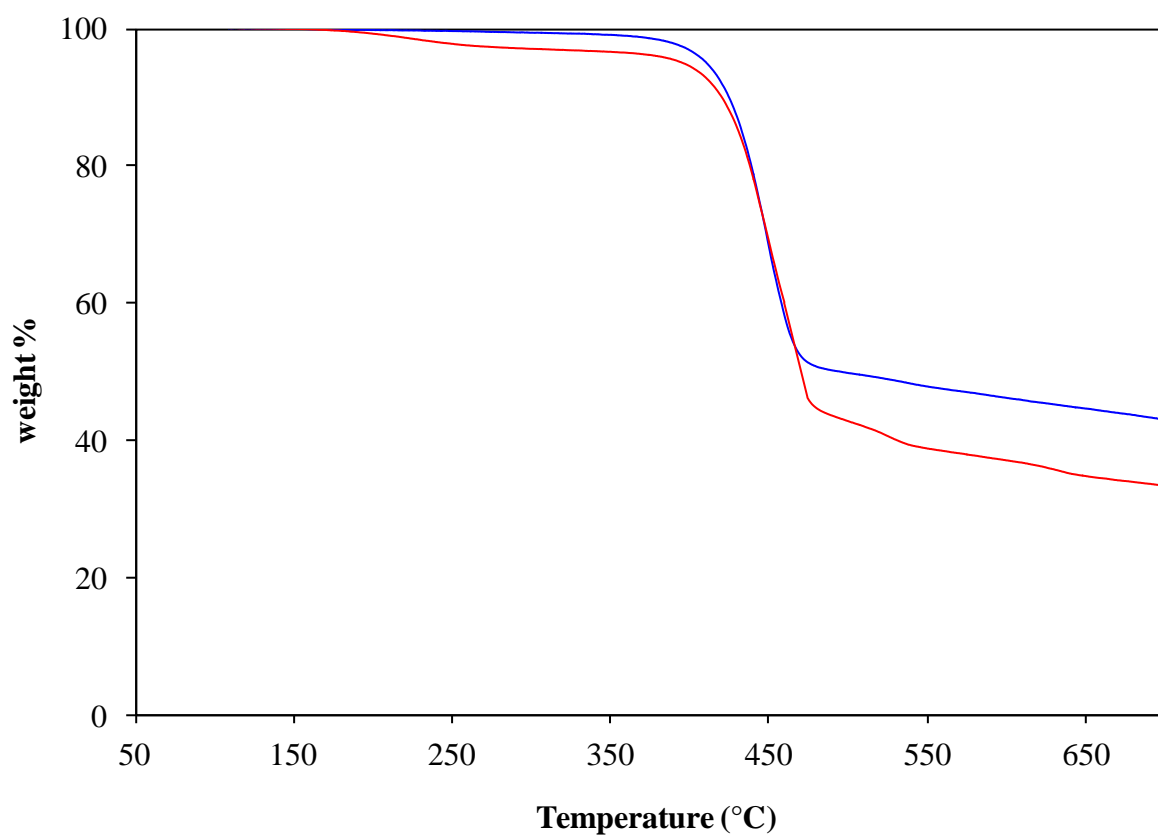


**Figure 2.** TGA curves of **PDI-2** (—) and **PDI-3**(—) under inert atmosphere  
(TGA curve for PDI-1 was reported in literature [2])

## Computational details

A computational study was carried out on structures and energies of **PDI-2** and **PDI-3**. To reduce the conformational space, long alkyl branched chains at the imide positions have been replaced by methyl groups. All calculations were performed with the GAMESS-US suite of programs [3]. Stable low energy conformations were obtained by density functional theory (DFT)[4] calculations. In particular, the B3LYP hybrid functional[5] and the standard 6-31G\*\* basis set were adopted. In order to scan properly the potential energy surfaces (PESs), different starting guess geometries were considered and fully minimized at the B3LYP/6-31G\*\* level of the theory. At this level of theory, the larger system consists of xx atoms, yy electrons and zz gaussian basis functions. A vibrational analysis was performed at the B3LYP/6-31G\*\* level on optimised geometries, where a lack of imaginary frequencies confirmed that they represent minimum-energy structures.

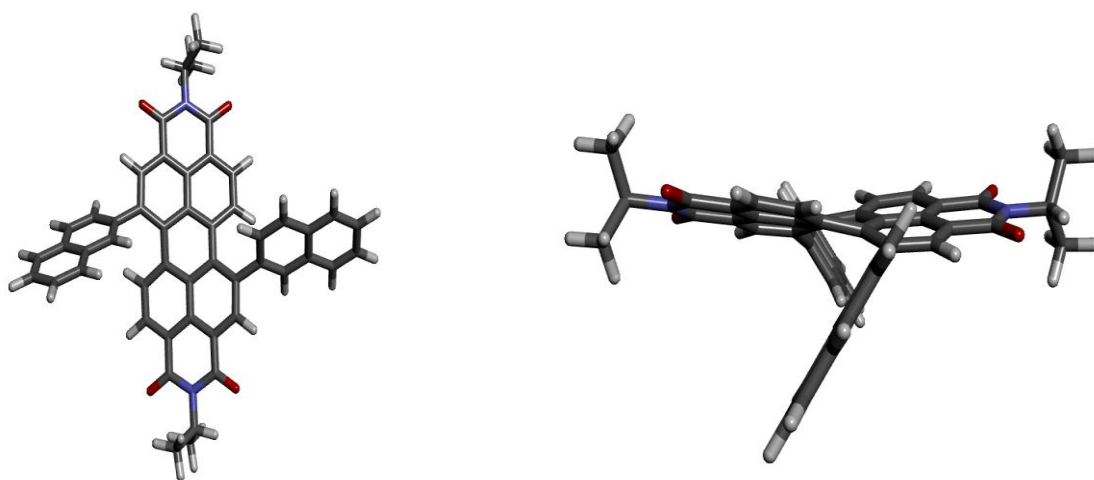


**Figure 3.** Two views of the absolute minima of **PDI-2** structure obtained at the B3LYP/6-31G\*\* level

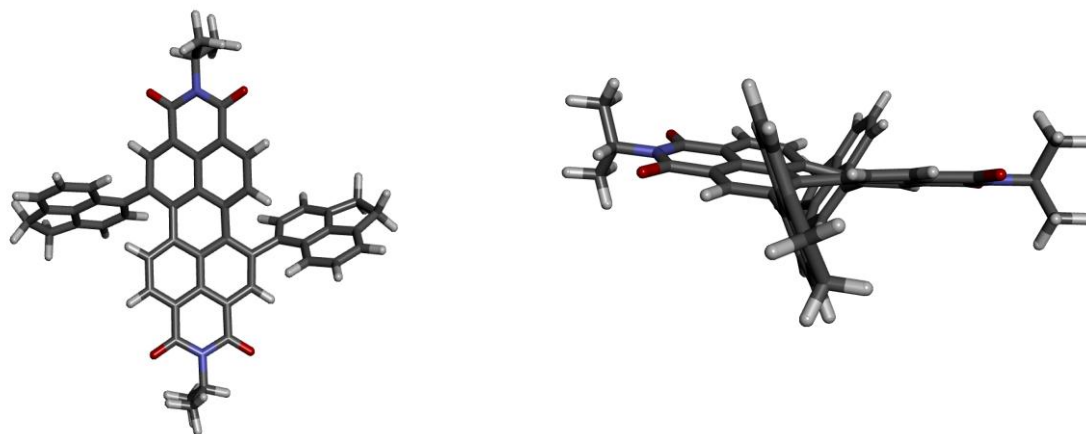
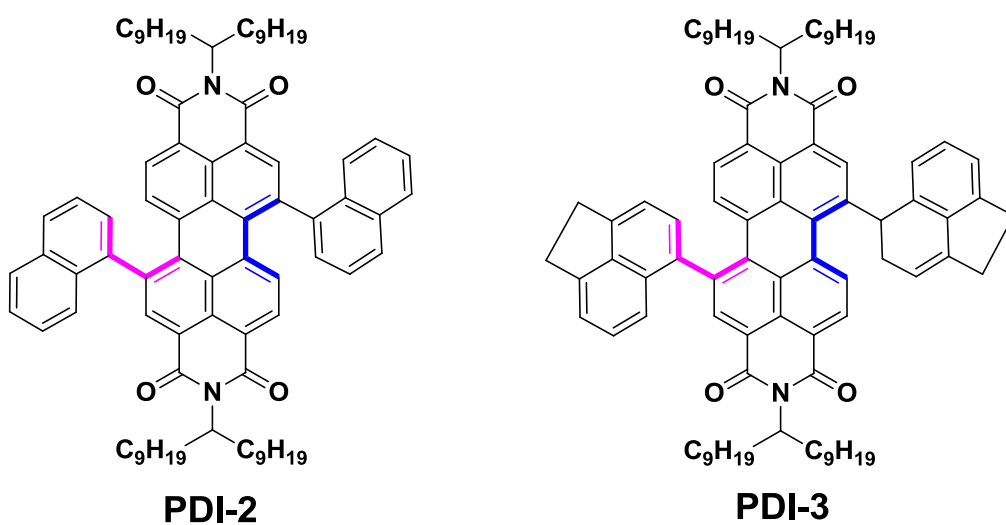


**Figure 4.** Two views of the absolute minima of **PDI-3** structure obtained at the B3LYP/6-31G\*\* level

Dihedral angles



Sample	Perylene plane dihedral angle (blue)	Substituent-peryene dihedral angle (pink)
<b>PDI-2</b>	19°	55°
<b>PDI-3</b>	19°	63°

## DSC of PDIs

The DSC data shown in Figure 3 are from the cooling (dashed line) and second heating (solid line) cycle.

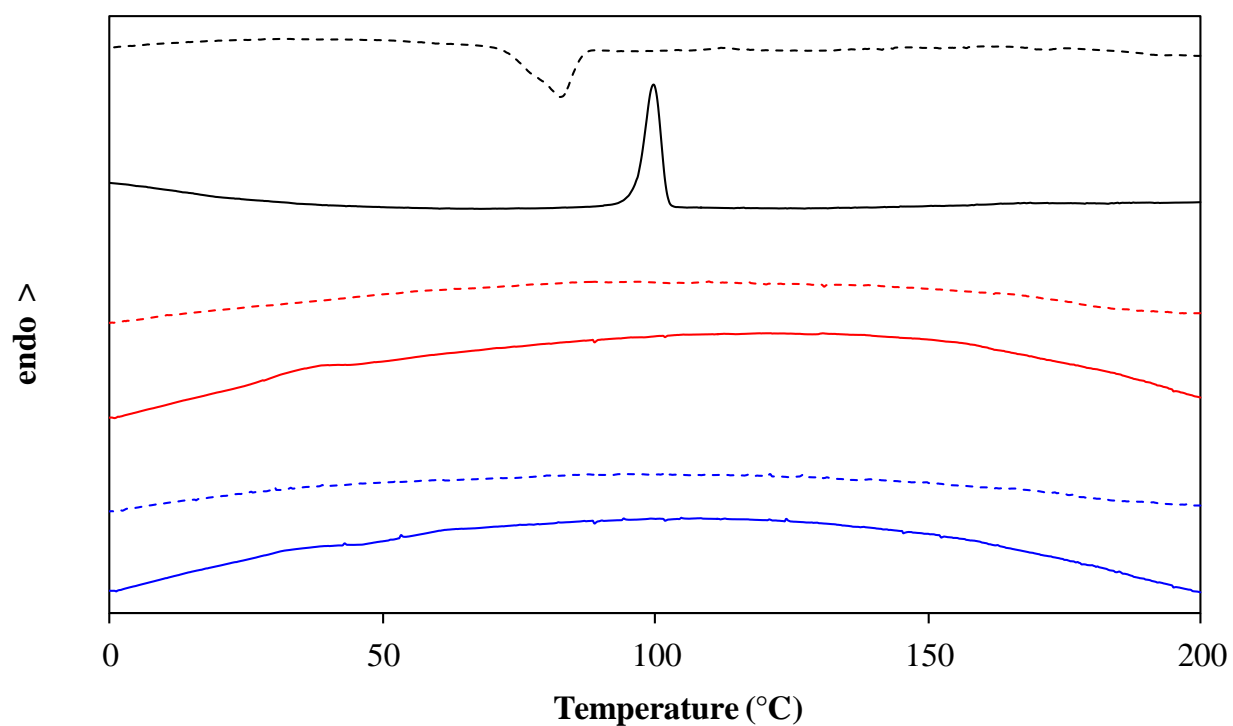


**Figure 5.** DSC thermograms of **PDI-1** (—), **PDI-2** (—) and **PDI-3** (—)

## Extinction coefficients and UV-Vis absorption spectra of PDIs in $\text{CHCl}_3$ solutions

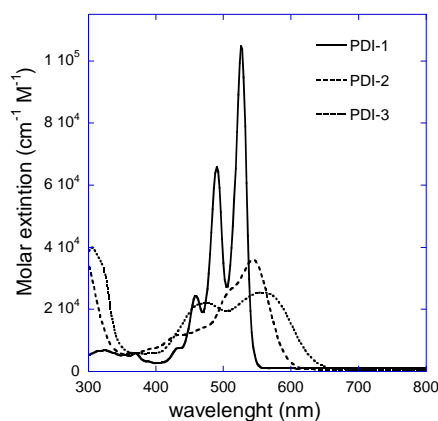


**Figure 6.** Molar extinctions for PDIs in  $1.25 \times 10^{-4}$  M solutions in  $\text{CHCl}_3$

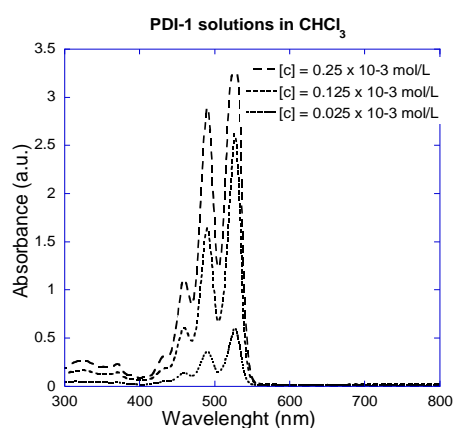


**Figure 7.** UV-Vis absorption of PDI-1 with different concentrations in  $\text{CHCl}_3$

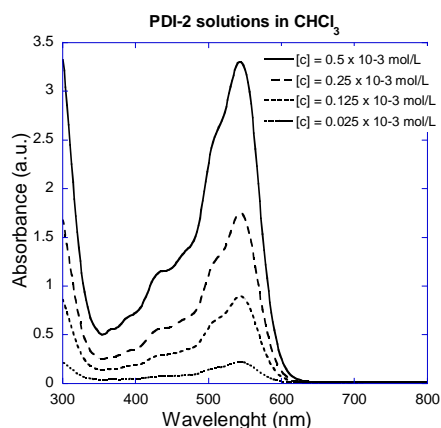


**Figure 8.** UV-Vis absorption of PDI-2 with different concentrations in  $\text{CHCl}_3$

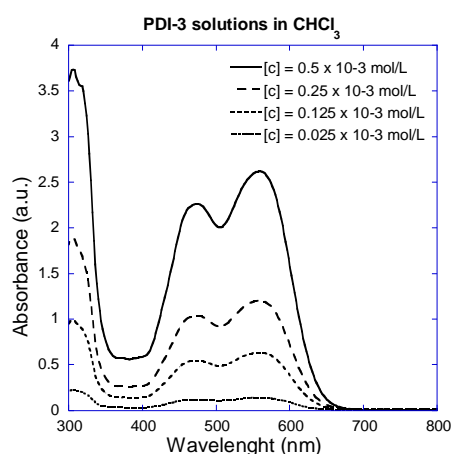


**Figure 9.** UV-Vis absorption of PDI-3 with different concentrations in  $\text{CHCl}_3$



### Cyclic voltammetry of **PDI-2** and **PDI-3**

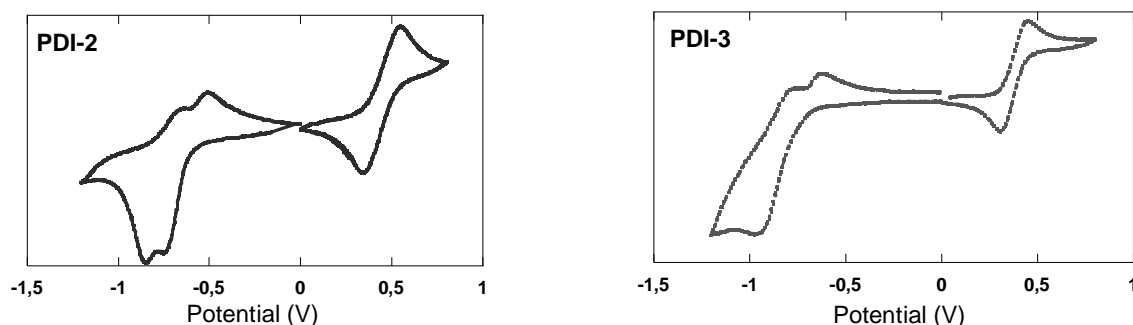


**Figure 10.** Cyclic voltammograms of **PDI-2** and **PDI-3** thin films

Photoluminescence spectra of pristine P3HT, PDIs and P3HT:PDIs (1:2 w:w) blends

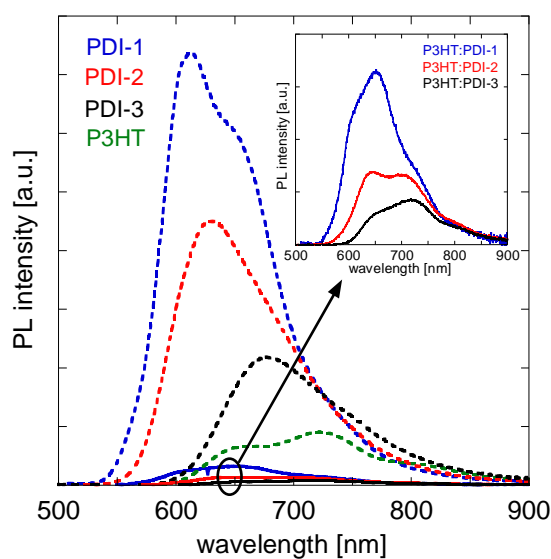


**Figure 11.** PL spectra of pristine component films (dashed lines) and optimized (1:2 w:w) P3HT:PDIs blends [presented on fig.3 in the main article text] (solid lines). The spectra are normalized to the number of absorbed photons at the incident excitation wavelength (488 nm).

## Optical microscopy



**Figure 12.** Optical microscopy of PDI-1, PDI-2 and PDI-3 films

## UV-Vis absorption spectra of optimized (1:2 w:w) P3HT:PDIs blends

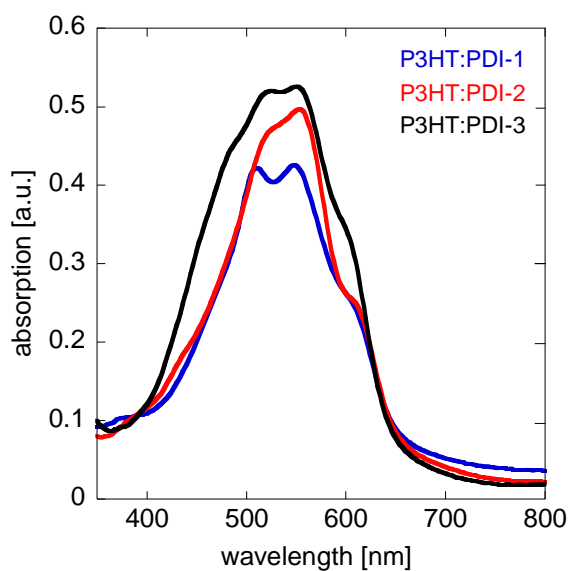


**Figure 13.** Absorption spectra of optimized blends [presented on fig.3 in the main article text] of P3HT:PDI-1 (from CB solvent -140nm thick), P3HT:PDI-2 and P3HT:PDI-3 blends (from oDCB solvent - 100nm and 110nm thick, respectively).

## Fabrication and characterization of solar cells

Solar cells were made with the conventional geometry glass/ITO/PEDOT-PSS/P3HT:PDI/Ca/Al in a MBraun drybox. Each ITO-glass substrate,  $15 \Omega/\square$ , purchased from KINTEC Company, was washed in ultrasonic bath at  $55^\circ\text{C}$ , sequentially with water, acetone and isopropanol. Then PEDOT:PSS (H.C. Starck, Clevios P VP Al 4083) was spin coated and dried on a hot plate  $100^\circ\text{C}/5 \text{ min}$ , to obtain the thickness of about 60 nm. The active layers were spin-coated from chlorobenzene (CB) or o-dichlorobenzene (oDCB) solution of P3HT:PDI 1:2 weight ratio (20 mg/ml or 25 mg/ml, respectively), with a thickness of about 100-140 nm. When chlorobenzene was used, after the active layer deposition, an optimal thermal annealing processing has been done at  $150^\circ\text{C}/5\text{min}$ ,  $150^\circ\text{C}/30\text{min}$ ,  $120^\circ\text{C}/5\text{min}$  for P3HT:PDI-1, P3HT:PDI-2 and P3HT:PDI-3, respectively. In the case of o-dichlorobenzene solvent, after the deposition, the active layer was solvent annealed by slow drying under a Petri dish (about 10h). After that, a mild thermal treatment of  $90^\circ\text{C}/10 \text{ min}$  has been done to remove the residual solvent. In all cases the thermal treatment has been done prior to the cathode deposition. The optimized cathode Ca(10nm)/Al(100nm) were deposited thermally through a  $6\text{mm}^2$  shadow mask in a vacuum chamber at a pressure of  $2 \times 10^{-6}$  mbar. All the thicknesses were measured with profilometer Dektak XT.

The current density–voltage measurements were performed directly in the glove box where the cell was assembled and annealed, with a Keithley 2602 source meter, under a 1 sun, AM1.5G spectrum obtained from an ABET Technologies solar simulator. EQE spectral responses were recorded by dispersing a Xe lamp through a monochromator, using a Si solar cell with calibrated spectral response to measure the incident light power intensity at each wavelength. The devices were taken outside the glove box for the EQE measurements, after mounting them on a sealed cell to avoid moisture and oxygen exposure. Photoluminescence (PL) spectra were recorded at room temperature, using 488 nm light excitation from a Xe lamp and a monochromator coupled to a CCD detector. The PL spectra of each film, have been normalized to the fraction of incident absorbed photons, to scale roughly as the emission yields.

# Photovoltaic characteristics of 1:2 P3HT:PDI (other solvents)

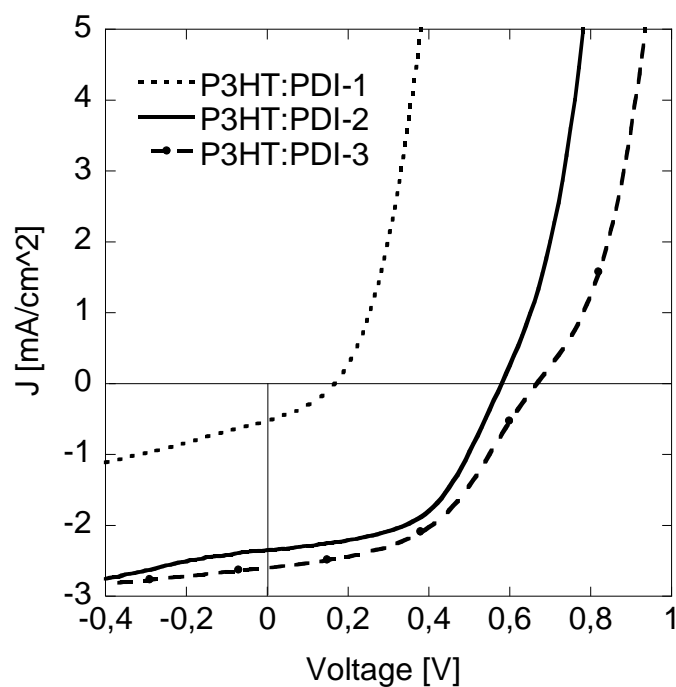


**Figure 14.** P3HT:PDI (1:2 w:w) device characteristics. J-V curves under AM1.5 G solar simulation, at 100 mW/cm<sup>2</sup>

Sample	V <sub>oc</sub> [V]	FF [%]	J <sub>sc</sub> [mA/cm <sup>2</sup> ]	PCE [%]
<b>P3HT:PDI-1</b>	0.17	0.34	0.51	0.03
<b>P3HT:PDI-2</b>	0.58	0.53	2.34	0.72
<b>P3HT:PDI-3</b>	0.67	0.47	2.59	0.82

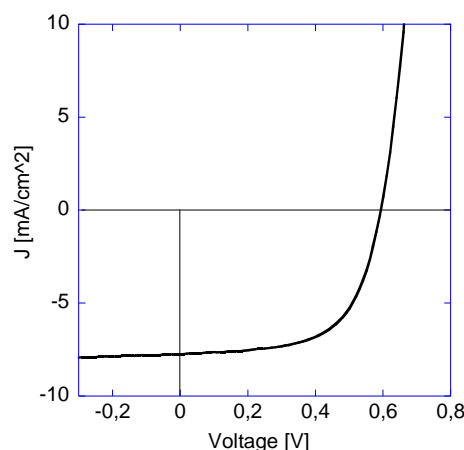
Conditions:

P3HT:PDI-1: active layer deposited from o-dichlorobenzene

P3HT:PDI-2: active layer deposited from chlorobenzene

P3HT:PDI-3: active layer deposited from chlorobenzene

## Photovoltaic characteristics of 1:1 P3HT:PCBM



Sample	V <sub>OC</sub> [V]	FF [%]	J <sub>SC</sub> [mA/cm <sup>2</sup> ]	PCE [%]
P3HT:PCBM	0.60	0.62	7.84	2.92

**Figure 15.** P3HT:PCBM device characteristics. J-V curves under AM1.5 G solar simulation, at 100 mW/cm<sup>2</sup>

### References

1. Erika Kozma, Dariusz Kotowski, Fabio Bertini, Silvia Luzzati, Marinella Catellani, *Polymer*, 2010, **51**(11), 2264
2. W. S. Shin, H.-H. Jeong, M.-K. Kim, S.-H. Jin, M.-R. Kim, J.-K. Lee, J. W. Lee, Y.-S. Gal, *J.Mater. Chem.*, 2006, **16**, 384.
- [3] a) M. W. Schmidt, K. K. Baldridge, J. A. Boatz, S. T. Elbert, M. S. Gordon, J. H. Jensen, S. Koseki, N. Matsunaga, K. A. Nguyen, S. Su, T. L. Windus, M. Dupuis, J. A. Montgomery, *J. Comput. Chem.*, 1993, **14**, 1347; M. S. Gordon, M. W. Schmidt, "Theory and Applications of Computational Chemistry, the first forty years", C. E. Dykstra, G. Frenking, K. S. Kim, G. E. Scuseria (editors), Elsevier, Amsterdam, 2005, p. 1167-1189.
- [4] a) R. G. Parr, W. Yang, "Density Functional Theory of Atoms and Molecules", Oxford Scientific, 1989; b) W. Koch, M. C. Holthausen, "A Chemist's Guide to Density Functional Theory", Wiley VCH, 2001; c) F. Jensen, "Introduction to Computational Chemistry", Wiley and Sons, Chichester, 2007.
- [5] a) A. D. Becke, *J. Chem. Phys.*, 1993, **98**, 5648; b) P. J. Stephens, F. J. Devlin, C. F. Chablonwski, M. J. Frisch, *J. Chem. Phys.*, 1994, **98**, 11623; c) R. H. Hertwig, W. Koch, *Chem. Phys. Lett.*, 1997, 268, 345.